Nucleic Acids Research, 1996, Vol. 24, No. 11 **2183–2189**

Molecular weight determination of plasmid DNA using electrospray ionization mass spectrometry

Xueheng Cheng[1,+], David G. Camp II[2], Qinyuan Wu[1], Ray Bakhtiar[1,§], David L. Springer[3], Brendt J. Morris[3,¶], James E. Bruce[1], Gordon A. Anderson[1], Charles G. Edmonds[1,3] and Richard D. Smith[1,*]

[1]Environmental Molecular Sciences Laboratory, Pacific Northwest National Laboratory, Richland, WA 99352, USA, [2]Department of Chemistry, Eastern Oregon State College, La Grande, OR 97850, USA and [3]Biology and Chemistry Department, Pacific Northwest Laboratory, Richland, WA 99352, USA

Received June 26, 1995; Revised November 3, 1995 and Accepted April 11, 1996

ABSTRACT

Ionization and molecular weight (MW) determination of megadalton size plasmid DNA has been achieved using electrospray ionization (ESI) with Fourier transform ion cyclotron resonance (FTICR) mass spectrometry. DNA molecules were shown to remain intact through electrospray ionization by collection on a specially prepared surface, followed by agarose gel electrophoresis. Individual highly charged ions of plasmid DNA produced by ESI were trapped in an FTICR cell for up to several hours and reacted with acetic acid to induce charge state shifts. Measurements of mass-to-charge ratios for these multiple peaks arising from charge state shifting give MW measurements of individual ions with an average accuracy of 0.2%. The MW distribution was obtained by measurements for a number of individual ions from the same sample [plasmid DNA: pGEM-5S MW(cal) = 1.946 MDa], yielding a MW(obs) of 1.95 ± 0.07 MDa for ions clustered in the vicinity of the expected MW.

INTRODUCTION

Mass spectrometry (MS) is the most accurate method for molecular weight (MW) measurement of relatively small molecules, and is widely used for identification and in structural determination. The development of matrix-assisted laser desorption ionization (MALDI) (1) and electrospray ionization (ESI) (2,3) now allow routine MS measurements of biopolymers of as large as 100–500 kDa. The ESI technique is especially gentle, generally producing multiply charged ions of intact molecules. Mass accuracies of ~0.01% can be obtained using conventional mass spectrometers (2,3) due to the generally limited mass-to-charge ratios (m/z) of the multiply charged ions. Ionization and detection of molecules in the megadalton range by ESI was reported in early work (4), but no confirmation was possible due to the inability to resolve distinct charge states as needed for MW determination. Recently the ultra-high resolving power (>10^6) (6–8) possible with electrospray ionization–Fourier transform ion cyclotron resonance (ESI–FTICR) (9,10) has allowed low p.p.m. accuracy mass measurements of biomolecules in the 5–70 kDa range (6–8). However, MW measurements for larger (>100 kDa) molecules remains difficult using this approach due to limitations upon the number of charges that can be usefully contained in the FTICR cell (9). The insufficient population for multiplets of charge states and isotope peaks prevents the assignments of the charge states *(z,* and hence the mass, *m)* since mass measurement for multiply charged ions requires the determination of *m/z* spacings between either different charge state peaks (11), isotope peaks (12) or peaks due to adducts (having known mass) (13).

We have recently developed methods for MW measurements of megadalton molecules based on the measurements of individual multiply charged ions using FTICR (14–16). Our approach involves the manipulation of individual ions (i.e., single ionic species) trapped in an FTICR cell. The large number of charges for large molecules provides sufficient sensitivity for individual ion detection (9,15). Stepwise charge state shifting of individual ions in reaction with selected reagents produces multiple peaks from the same ion from which charge states and MW can be calculated (14–16) as:

$$MW = [(m/z)_1 \pm A][(m/z)_2 \pm A]/\Delta(m/z)$$

Where $(m/z)_1$ and $(m/z)_2$ are the mass-to-charge ratios measured before and after the charge state shifting reaction, $\Delta(m/z) = (m/z)_2 - (m/z)_1$, and A is the mass of the charge-carrying species (A is negative for an adduct and positive when the mass A is removed from the molecule). It should be noted that in a recent report we also described an alternative approach for charge determination of very large individual DNA ions (up to 10^8 Da) based on the measurement of the induced current (and thus the charge) of an individual ion in the FTICR detection circuitry, but at present this approach offers lower precision (5–10%) (17).

Analysis of an ensemble of ions can, in principle, yield the MW distribution, in essence, a 'mass spectrum' can be constructed one

* To whom correspondence should be addressed

Present addresses: +Pharmaceutical Discovery Division, Abbott Laboratories, Abbott Park, IL 60064, USA, §Drug Metabolism, Merck Research Laboratory, PO Box 2000, Rahway, NJ 07065, USA and ¶Los Alamos Technical Associates, Inc., 8633 Gage Boulevard, Kennewick, WA 99336, USA

(individual) ion at a time yielding the MW distribution through measurements of a large number of individual ions. We have performed such measurements for a 3126 bp plasmid molecule, pGEM-5S. This plasmid DNA was chosen for these initial studies due to its unique topomeric characteristics which facilitated purification and allowed highly specific characterization of the material on the basis of sedimentation velocity and electrophoretic mobility for comparison with ESI–FTICR results.

MATERIALS AND METHODS

Preparation of plasmid DNA

Plasmid molecules pGEM-5S, a 3126 bp supercoiled closed circular double-stranded plasmid subclone of pGEM-9Z-f(–) which includes the 5S ribosomal RNA gene from *Xenopus borealis* (18), were prepared and purified to eliminate contamination by lower mass DNA, ribonucleic acid and salts. The plasmid had a predicted MW of 1 945 664 Da for the free acid calculated from the base sequence (18). The plasmid was cultured in transformed *Escherichia coli* JM109 and, following alkaline lysis, the supercoiled DNA was separated by CsCl density gradient centrifugation. Successive 100% ethanol precipitation from ammonium acetate solution was followed by ultrafiltration with Centricon-100 (Amicon, Danvers, MA). Preparations consisted principally of the supercoiled species, with small contributions by nicked circular and linearized plasmid.

Electrophoresis of electrosprayed plasmid DNA

The fate of plasmid upon electrospray ionization was investigated by collection of samples on conductive surfaces followed by agarose gel electrophoresis analysis (5). Targets consisted of a chemically clean stainless steel foil or aqueous 9 mM Tris, 9 mM boric acid and 0.2 mM EDTA (TBE) buffered droplet (50 µl) stabilized by 1% agarose gel. The plasmid (10 µg/µl in deionized water) was delivered to the ion source at 0.2–0.5 µl/min, and the targets were placed in atmospheric pressure at entrance plate of the ESI–MS interface (see below) under otherwise identical conditions for the ESI–MS experiments described next (i.e., in the presence of sheath gas and counterflow gas, as well as differential pumping behind the plate). After drying of the target, the plasmid was extracted into 50 µl of TBE buffer. Electrophoretic analysis of the recovered plasmid samples was in 1% agarose gels buffered in TBE with visualization by ethidium bromide (0.5 µg/ml).

Mass spectrometry

Initial ESI–MS experiments were performed using a Sciex (Thornhill, ON, Canada) TAGA 6000E triple-quadrupole mass spectrometer with a resolving power (m/Δm) of ~800 and mass range of 1400 (*m/z*). This instrument was equipped with a prototype ESI source having a nozzle-skimmer interface (19). For collection of plasmid samples and for acquiring plasmid DNA mass spectra, the following parameters were used: 10 µM DNA samples in deionized water; sample infusion rate of 0.2 µl/min; spray voltage of –2.5 kV; nozzle voltage of –60 V; skimmer voltage of –150 V. Coaxial flows SF_6 and countercurrent N_2 were employed for the ESI of DNA samples.

FTICR experiments were performed using a modified IonSpec (Irvine, CA) FTICR with an Oxford 7-Tesla superconducting magnet, and incorporating a modified Analytica (Branford, CT) ESI source (7). Time domain signal acquisition was accomplished using an Omega data system (version 3.0) and a separate, home-built, extended time domain data acquisition system (8,15). The plasmid DNA sample was prepared as described above with a final concentration of 0.2 mg/ml (0.1 µM) in deionized water. The sample was electrospray as above, and ions were accumulated in the FTICR cell for 1 s at ~10^{-4} Torr (nitrogen), collisionally cooled for 15 s and detected using chirp excitation (sweep rate 35 Hz/µs) and broadband data acquisition (using a sampling rate 200 kHz) for 40 s (7). For mass and charge determination, the gas phase reaction of individual DNA ions with acetic acid was used to induce charge state changes. Mass spectra were acquired several minutes after the pulsed addition of acetic acid to the system (which raised the system pressure from 10^{-9} to 10^{-7} Torr for several seconds) (15), which was found to facilitate charge transfer reactions at the desired rate.

RESULTS

Analysis of plasmid DNA on quadrupole mass spectrometer and characterization of DNA after ESI

At the low mass spectrometric resolution of a quadrupole mass spectrometer, ESI of the plasmid DNA sample afforded a single broad envelope of ionized species extending between *m/z* 500 and 1400 (the upper *m/z* of the instrument). Maximum relative abundance was found at *m/z* ~700 (Fig. 1) (5). This observation suggests the possible production of gas-phase multiply charged molecular anions of the plasmid, but affords no useful mass measurements since both the mass and charge are unknown. We further characterized the behavior of the plasmid by electrospraying the nucleic acid onto targets of stainless steel foil or Tris–EDTA–Borate (TEB) buffer droplets stabilized by 1% agarose gel. After being electrosprayed onto these targets, the plasmid was extracted with TEB buffer and examined by 1% agarose gel electrophoresis (Fig. 2). When electrosprayed onto a dry stainless steel target, the plasmid was substantially altered, with the production of a wide range of materials of both higher and lower electrophoretic mobility. However, when the plasmid was electrosprayed onto a liquid buffer surface, the plasmid remained substantially intact, with the closed circular form of the nucleic acid opened to the nicked circular form. No substantial degradation to material of lower mass was observed. On the basis of these results, it cannot be determined whether the nicked circular form resulted from the ESI process, the surface deposition, or subsequent handling prior to electrophoresis. Regardless, these results indicate that the plasmid DNA is at least substantially intact after being electrosprayed, and the actual MW measurements using FTICR described below, confirms the stability of at least some substantial fraction of the double-stranded megadalton nucleic acids through the initial electrospray process and FTICR measurements.

Analysis of plasmid DNA on FTICR–MS

In our ESI–FTICR experiments of plasmid DNA in the negative ion mode, multiple deprotonation of phosphodiesters produced ions having a broad *m/z* distribution, similar to the low resolution quadrupole experiments except that ions appeared at somewhat higher *m/z* in FTICR mass spectra (an observation that may be due to the different ESI–MS interfaces used, or to a greater extent

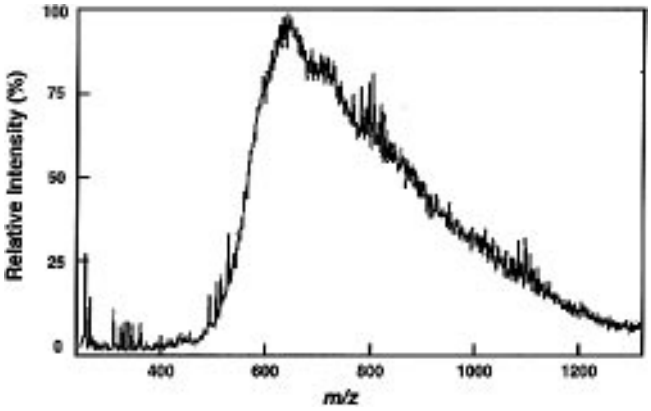

Figure 1. ESI-MS spectrum of plasmid DNA pGEM-5S acquired on a quadrupole mass spectrometer.

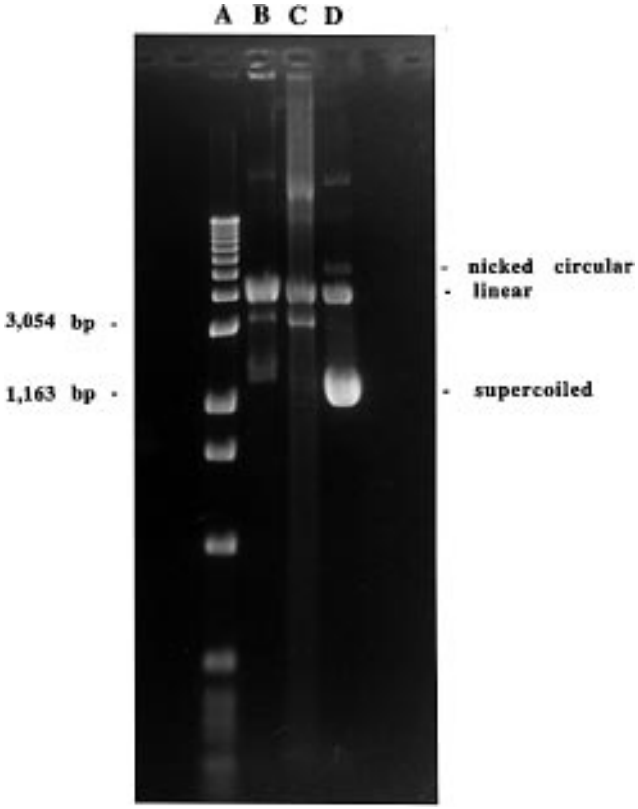

Figure 2. One percent agarose gel electrophoresis of (**A**) DNA ladder (1 kb) (Bethesda Research Labs); (**B**) electrospray ionization preparation of pGEM-5S onto a target consisting of a droplet of TEB buffer stabilized by 1% agarose gel; (**C**) electrospray ionization preparation of pGEM-5S onto a target of chemically clean stainless steel foil; and (**D**) the control pGEM-5S preparation.

of charge reduction due to the much longer time before analysis). The FTICR mass spectra consist of a multitude of narrow peaks with no clear pattern of charge states (or isotopic peaks), and having a pattern which varies with each subsequent injection of ions. The evidence that those narrow peaks are due to individual ion contributions includes the observation of quantized behavior of those ions in responding to RF excitation, ejection and reaction, and the results of the time-resolved ion correlation (TRIC) experiments, as described previously (15). An accurate MW measurement cannot be obtained directly from these spectra, despite the ultra-high resolution capability of the instrument, since the charge states of the ions are unknown. By reducing the ion population using recently described techniques (14–16), these individual ions can be clearly identified (Fig. 3). Through repeated application of these ion population trimming techniques, we typically obtained populations of 1–20 individual ions, suitable for subsequent ion–molecule reaction experiments. Each ion can be observed with a signal-to-noise ratio of ~20–40:1 due to their large charge (15). The presence of trace amounts of gaseous acetic acid induced successive charge state shifts in *m/z* of individual ions during the course of time-domain acquisitions extending to as long as 40 s. The *m/z* shifting is revealed by performing segmented Fourier transformation of the full time domain signal and/or extraction of the individual ion time-domain signal (time-resolved ion correlation-TRIC) (15), allowing the reactant–product relationship between peaks to be established. Figure 4 shows TRIC stack plots for two individual ions from pGEM-5S DNA, illustrating this temporal behavior. During an acquisition period of 6 s, the *m/z* of one ion moved twice with approximately equal displacements (Fig. 4A), while another ion shifted four times (Fig. 4B). We have observed an individual ion shifting its *m/z* position up to 12 times during the course of a time domain acquisition period of 27 s (data not shown). Some of the peaks in Figure 4 are also split or broadened due to additional *m/z* shifts of much smaller size. The larger *m/z* shifts evident in Figure 4 are identified as charge state changes induced by either reaction with acetic acid (equation **1**) or dissociative proton transfer of a DNA–acetic acid complex formed through otherwise non-reactive collisions (equation **2**). Similar proton transfer reactions of multiply protonated biomolecular ions have been studied previously (16,20). The smaller *m/z* shifts are attributed to addition/elimination of neutral molecules (e.g., acetic acid) (equation **3**). The likely origin of the small *m/z* shifts can be tentatively assigned based on the values of the charge state shifts which give the approximate charge number (*z*) of the peaks, which in turn allow calculation of the masses of the neutral species involved in the small *m/z* shifts.

$$M^{n-} + CH_3COOH \rightarrow M^{(n-1)-} + CH_3COO^- \quad \mathbf{1}$$

$$M^{n-}(CH_3COOH) \rightarrow M^{(n-1)-} + CH_3COO^- \quad \mathbf{2}$$

$$M^{n-} + CH_3COOH \leftrightarrow M^{n-}(CH_3COOH) \quad \mathbf{3}$$

The small regularly-spaced *m/z* shifts were not observed when nitrogen gas was added instead of acetic acid. We also observed that the reactivity of individual DNA ions changes with their *m/z* value, i.e., ions with higher *m/z* are generally less reactive toward charge state shifting. This *m/z* dependent reactivity is qualitatively ascribed to differences in the contribution of Coulombic (repulsive) forces to the reaction energetics for multiply charged ions of different *m/z* (16,20).

Origins other than charge state changes for the larger *m/z* shifts observed are considered very unlikely. For example, if the observed *m/z* shift were due to addition of N_2, then the MW of the ions would have to be ~34 000 Da (inconsistent with the high S/N observed, which indicates a very high charge and mass since signal intensity is approximately proportional to ion charge; 15). Alternatively, the mass of a neutral adduct would have to be ~1700 Da, if the ion mass were assumed to be ~2 MDa, to result

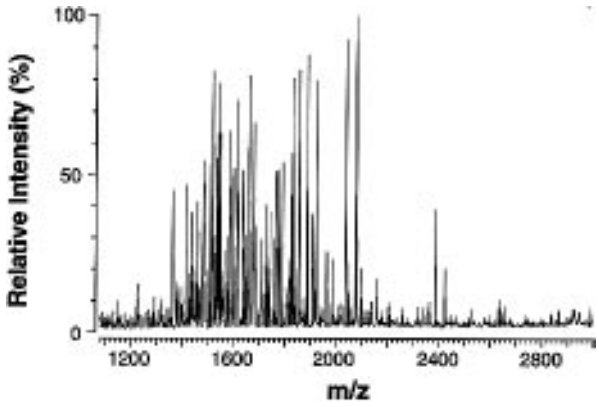

Figure 3. ESI-MS spectrum of plasmid DNA pGEM-5S acquired on an FTICR mass spectrometer showing individual ions after repeated application of ion population trimming techniques.

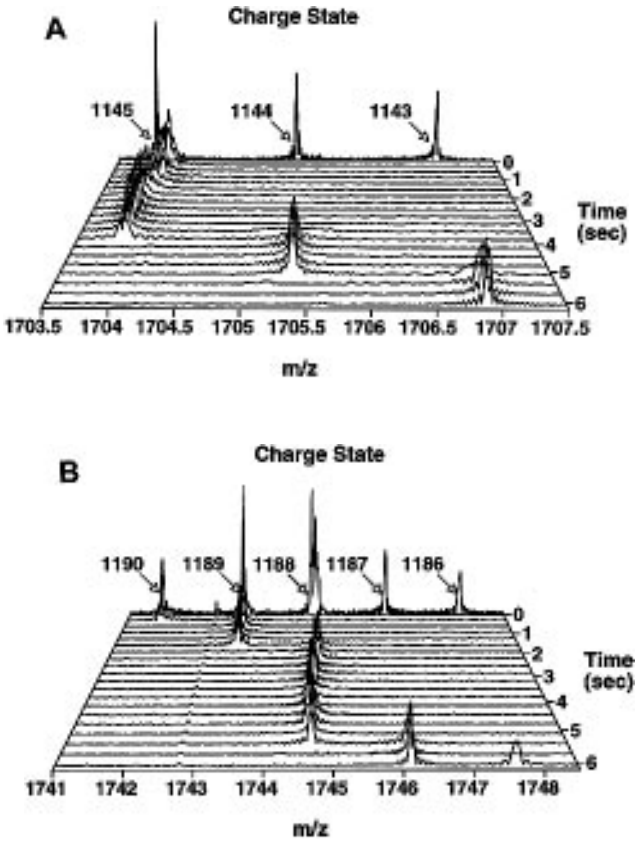

Figure 4. Stack plots of mass spectra of pGEM-5S plasmid DNA in the range of (**A**) *m/z* 1701–1708 and (**B**) *m/z* 1740–1749. The stack plots are produced by successive Fourier transformation of small segments of time domain data (128k data increments, 64k step size). The mass spectra were acquired with chirp excitation (sweep rate 35 Hz/μs) and broad band data acquisition (sampling rate 200 kHz) for 40 s. The plot at time zero is the result of Fourier transformation of the entire time domain data.

in the observed *m/z* shifts. It is implausible that neutral molecules of such high mass and with high enough number density exist in the vacuum for such a reaction to occur with the observed frequency. The distinctive and step-wise *m/z* shifts, observed only when acetic acid was added, and the distinctive TRIC behavior (14,15) constitutes the strongest evidence for the assignments for their origin. Reactions of acetic acid with gas phase DNA ions other than equations **1**–**3** (such as cleavage of backbone and elimination of nucleobases), although possible at elevated collision energies or in the ESI source (21,22), are unlikely under the FTICR conditions used in this work. Indeed, recent work has shown that even fragile noncovalent complexes produced by ESI can be effectively trapped, stored and analyzed under similar experimental conditions (23,24). We have separately investigated charge state reduction of small oligonucleotide negative ions induced by various acids (including acetic acid) added to the solution (25). No reaction other than proton transfer (charge reduction) was observed, even under much harsher (i.e., more energetic) ESI interface conditions (25). The observation in this work that DNA ions with *m/z* values >2200 primarily undergo a series of small shifts, instead of larger shifts shown in Figure 4, is also consistent with the larger shifts being due to charge state changes and the small shifts being due to addition/elimination of a neutral reagent. The low *m/z* ions (of the same mass) carry more charges and are thus more reactive towards proton transfer reaction (equation **1**) than the high *m/z* ions. These different reactivities are analogous to that observed for multiply protonated proteins in the gas phase (20).

When the successive charge state shifts arise from exchange of a specific charge carrier species (e.g., H^+), the mass and charge of the ion can be uniquely determined with the assumption that each shift is due to exchange of one charge. The ion giving rise to the spectrum shown in Figure 4A can have its mass and charge calculated with a precision of 0.1% (Table 1). However, when neutral addition/elimination occurs concurrently with charge state shifting, the number of neutral species involved in each shifting event needs to also be determined if high precision mass measurement is to be obtained. An example is shown in Figure 4B and lower portion of Table 1 where the first *m/z* shift (1.627) is larger than the second shift (1.373). The difference (0.254) corresponds to ~301 Da, which is consistent with loss of five HOAc molecules during the second charge state shifting event. It should be noted that only the ratio of the number of neutrals involved in different charge state shifting events is uniquely determined. For example, if only one charge state shift is observed, the number of accompanying neutral addition/elimination cannot be unambiguously determined in the absence of constraints upon chemical composition of the adducts. We thus assumed minimum neutral involvement in our interpretation of charge state shifting results; i.e., no neutral addition/elimination is assumed unless clearly indicated by an inconsistency in the two adjacent *m/z* shifts. When only one charge state shift was observed during the time-domain acquisition, no neutral addition/elimination was assumed to take place. We have used a mathematical procedure to fit the observed *m/z* shifts to the charge states of the ions, the MW of the DNA and the number of neutral molecules involved through addition/elimination with each charge state shift. The fitting procedure involves finding the MW that minimize the χ^2 or 'sum of squares of deviations' (the differences between the calculated and observed *m/z*) for a initial guess of charge state. The charge state is then varied, and the one which gives minimum χ^2 is found allowing a best-fit MW to be calculated. For the charge state shifting process shown in equation

1 and the initial guess z_i (i = 1, 2, ... m, where m is the number of charge states observed), the best-fit MW value:

$$M_z = \Sigma[(B_i + A)/z_i]/\Sigma(1/z_i^2)$$

Where A is the mass of the charge-carrying species and $B_i = (m/z)_{i,obs}$. For a process involving simultaneous charge state shifting and addition of **n** neutral species with mass N:

$$M_z = \Sigma[(B_i + A)/z_i - \mathbf{n}N/z_i^2]/\Sigma(1/z_i^2)$$

The MW values that produce a χ^2 having twice that of the global minimum are reported as the range of uncertainties for the fitting. The effect of cyclotron frequency drift observed previously (8) is less than the uncertainty from this fitting procedure. The data listed in the lower portion of Table 1 shows the fitting results for the individual ion in Figure 4B, and yields an accuracy of 0.2%. The same procedure was applied to other individual ions and the MW distribution (histogram) for the pGEM-5S DNA samples is obtained from measurements of 62 individual ions (Fig. 5). An average MW of 1.95 ± 0.07 MDa was derived from the 'peak' representing the cluster of individual ions (out of 62) in the region of the expected molecular weight. These species are attributed to the plasmid DNA ions (Fig. 5), which has a theoretical MW of 1.946 MDa.

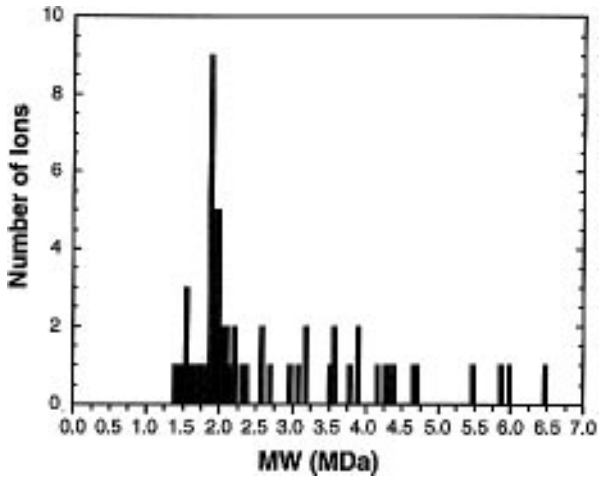

Figure 5. Histogram plot of MW distribution for pGEM-5S plasmid DNA. The vertical axis represents the number of ions observed in the MW range denoted by the horizontal axis. The average uncertainty in the MW determination of each of the individual ions was 0.2%.

Table 1. MW determination for two individual ions of pGEM-5S plasmid DNA from the measurement of charge state shifting upon reaction with acetic acid

z[a]	*m/z* (obs)	Δ(*m/z*)	MW (MDa)[b]
Data from Figure 4A			
1145	1703.902		1.952122
1144	1705.393	1.491	1.952123
1143	1706.886	1.493	1.952123
		Average MW	1.952123
		MW uncertainty	0.002[c]
Data from Figure 4B[d]			
1190	1741.668		2.073784
1189	1743.295	1.627	2.073796
1188	1744.668	1.373	2.073803
1187	1746.129	1.461	2.073792
1186	1747.549	1.420	2.073789
		Average MW	2.073793
		MW uncertainty	0.004[c]

[a]The number of charges on the individual ion, obtained using the fitting procedure described in the text.
[b]Calculated from the observed *m/z* and *z* values obtained from fitting.
[c]Uncertainty for the MW determination of the individual ion. The source of the uncertainties is primarily from the uncertainty in charge state determination (fitting).
[d]The number of neutral (acetic acid) addition used in the fitting is –3, 2, 0, 1 for charge state shifting steps with Δ(m/z) values of 1.627, 1.373, 1.461 and 1.420 respectively.

DISCUSSION

The measured MW for the principal species from the 'spectrum' shown in Figure 5 for pGEM-5S agrees well with the calculated MW (based on the base sequence; 18) within the experimental uncertainty. This observation indicates that at least a substantial portion of the plasmid DNA survives intact through the electrospray ionization process, transportation into FTICR cell, collisional trapping and detection. The observed dispersity of MWs for the individual ions, however, exceeds that expected for the samples based upon the reparation procedure described. For example, the spectral width (FWHM) for the theoretical isotope distribution is calculated to be only 76 Da for pGEM-5S plasmid DNA, and thus cannot account for the distribution. The lower mass species may also be a result of partial degradation of the sample during handling, however, electrophoresis results were not consistent with this explanation. In addition, it was clear that individual DNA could persist in the FTICR cell for hours without apparent dissociation. This indicates that after trapping, the temperature or the internal energy of the ions is low. Minor occurrences of fragmentation of individual DNA ions during remeasurements were observed when the radio-frequency (RF) excitation level for detection was increased substantially, causing energetic collisions of DNA ions with the background gas (or, less likely, a metal surface of the cell). It is possible that some dissociation occurred during the collisional trapping step, although we have now demonstrated that a wide range of noncovalent complexes formed by ESI can be trapped under similar trapping conditions (23). Thus, transport through the ESI interface is the most likely location for dissociation to occur; however, it should be noted that smaller (but much more fragile) noncovalent complexes have been effectively transported through the interface without dissociation (23). Recent work has also shown that PCR products of at least 105 bp size can be effectively studied using ESI–FTICR without detectable dissociation using similar experimental conditions (24). The apparent width to the major peak at ~1.95 MDa may be caused by different extents of residual salt adduction (Na^+, NH_4^+, etc.) and, to a lesser extent, of solvent and acetic acid added in the gas phase. The possibility of incomplete desolvation of DNA ions from ESI was evaluated by increasing the temperature of the heated capillary in the atmosphere-vacuum interface of the ESI–FTICR. No systematic changes in the measured MW were found, indicating that residual solvation is likely unimportant, and consistent with the

fact that residual solvation is rarely observed in our FTICR studies, even under the most gentle interface conditions (23,24). Another possible source of higher mass species is concatemer formation of the high copy number plasmid *in vivo*. These are observed as minor bands in the electrophoretic separation (Fig. 2). Such possible concatemer formation was also evident from the spectra of plasmid pUB110 (MW = 3 MDa), another DNA analyzed in this work (data not shown), but no substantial ion population is evident at exactly twice the plasmid mass as would be required by this explanation. Finally, we note that the MW distribution of species shown in Figure 5 more closely resembles the electrophoretic separation lane C (samples electrosprayed on to the stainless steel surface) than lane B (captured on the buffered liquid surface) in Figure 2, especially in the high MW region. Some dissociation during ion formation may be speculated as a possible source of these unknown contributions to the mass spectra, but further study is clearly required to determine their origin. One possibility is that same transient contact of the ions occurs with the heated (stainless steel) capillary inlet used in the ESI source, resulting in some contribution of products similar to that observed by collection on an unheated stainless steel surface.

The present results show that plasmid DNA can be ionized, detected and measured intact by ESI–FTICR, although a portion of the ions apparently undergo some reaction or degradation under the conditions used for this study. Since the original submission of this work, a low resolution time-of-flight study has been reported, also based upon single ion measurements, that is qualitatively consistent with the measurements summarized in Figure 5 (26). Even at the much lower precision of this work, some contributions to the spectra are noted at both higher and lower mass that are not readily explained (26).

It is feasible that improved sample handling or better desalting [e.g., on-line capillary electrophoresis (CE) or LC-MS] (27) might reduce some such contributions. Possible contributions due to residual solvation might also be eliminated by gas-phase 'drying' of DNA ions using low energy collisional activation or IR photo-activation (28). Despite this, a significant fraction of ions having MWs close (± 0.07 MDa) to that calculated were observed, and measured with good precision. The obtainable accuracy for mass determination of individual ions is much better than electrophoresis, 0.1% being feasible with multiple charge state shifts (and potentially <0.01%) (14,15). Further improvement in the accuracy of individual ion MW determination should be possible through greater precision of the charge state shifting measurements. The complication noted due to the neutral addition/elimination, may potentially be alleviated by performing charge state shifting experiments for ions of lower *m/z* that are more reactive and possibly less prone to neutral adduction. The complete elimination of sodium adduction for smaller oligonucleotides as recently been obtained using a new approach for on-line dialysis (29). Alternatively, MW measurements of individual ions could be achieved by photo-cleavage of built-in chromophores (of known mass) which will eliminate the need for neutral gas and will improve the mass measurement accuracy substantially.

The accurate MW determination of large biomolecules and complexes of large biomolecules has potential to contribute to the study of important genomic and cellular processes (30,31) such as the control of gene expression and the modulation of signal transduction. Accurate MW determination for large DNA is also vital to several proposed approaches to rapid DNA sequencing (32,33). In a more ambitious scenario, stepwise degradation from one terminus of an individual DNA ion may provide the basis for a rapid sequencing method. DNA mapping efforts could also benefit from a rapid and accurate MW determination of the large restriction fragments (34,35) without the need for cloning. Recent results indicate that much larger DNA fragments of >100 MDa (>150 kbp) may also be amenable to study (17). However, as shown in this work, further development is required in order for this technique to become practical and useful in the routine analysis of large biomolecules.

ACKNOWLEDGEMENTS

We thank Drs B. D. Thrall, S. A. Hofstadler, H. R. Udseth, A. L. Rockwood and M. G. Sherman for helpful discussions and technical assistance, S. Van Orden for calculating the isotope distribution for the plasmid DNA and the US Department of Energy Human Genome Program through the Director, Office of Health and Environmental Research and through PNNL internal Exploratory Research of Pacific Northwest Laboratory under Contract DE-AC06-76RLO 1830. D.G.C. II acknowledges partial support from Eastern Oregon State College. Pacific Northwest National Laboratory is operated by Battelle Memorial Institute.

REFERENCES

1 Karas, M. and Hillenkamp, F. (1988) *Anal. Chem.* **60**, 2299–2301.
2 Fenn, J. B., Mann, M., Meng, C. K., Wong, S. F. and Whitehouse, C. M. (1989) *Science* **246**, 64–71.
3 Smith, R. D., Loo, J. A., Loo, R. R. O., Busman, M. and Udseth, H. R. (1991) *Mass Spectrom. Rev.* **10**, 359–451.
4 Nohmi, T. and Fenn, J. B. (1992) *J. Am. Chem. Soc.* **114**, 3241–3246.
5 Edmonds, C. G., Springer, D. L., Morris, B. J., Thrall, B. D. and Camp, D. G. (1993) *Proceedings of the 41st ASMS Conference on Mass Spectrometry and Allied Topics* 272a–272b.
6 Beu, S. C., Senko, M. W., Quinn, J. P., Wampler, F. M. and McLafferty, F. W. (1993) *J. Am. Soc. Mass Spectrom.* **4**, 557–565.
7 Winger, B. E., Hofstadler, S. A., Bruce, J. E., Udseth, H. R. and Smith, R. D. (1993) *J. Am. Soc. Mass Spectrom.* **4**, 566–577.
8 Bruce, J. E., Anderson, G. A., Hofstadler, S. A., Winger, B. E. and Smith, R. D. (1993) *Rapid Commun. Mass Spectrom.* **7**, 700–703.
9 Marshall, A. G. and Grosshans, P. B. (1991) *Anal. Chem.* **63**, 215A–229A.
10 Henry, K. D., Williams, E. R., Wang, B. H., McLafferty, F. W., Shabanowitz, J. and Hunt, D. F. (1989) *Proc. Natl Acad. Sci. USA* **86**, 9075–9078.
11 Mann, M., Meng, C. K. and Fenn, J. B. (1989) *Anal. Chem.* **61**, 1702–1708.
12 Henry, K. D. and McLafferty, F. W. (1990) *Org. Mass Spectrom.* **25**, 490–492.
13 McLuckey, S. A., Glish, G. L. and Van Berkel, G. J. (1991) *Anal. Chem.* **63**, 1971–1978.
14 Smith, R. D., Cheng, X., Bruce, J. B., Hofstadler, S. A. and Anderson, G. A. (1994) *Nature* **369**, 137–139.
15 Bruce, J. E., Cheng, X., Bakhtiar, R., Wu, Q., Hofstadler, S. A., Anderson, G. A. and Smith, R. D. (1994) *J. Am. Chem. Soc.* **116**, 7839–7847.
16 Cheng, X. H., Bakhtiar, R., Van Orden, S. and Smith, R. D. (1994) *Anal. Chem.* **66**, 2084–2087.
17 Chen, R., Cheng, X., Mitchell, D. W., Hofstadler, S. A., Wu, Q., Rockwood, A. L., Sherman, M. G. and Smith, R. D. (1995) *Anal. Chem.* **67**, 1159–1163.
18 Thrall, B. D., Mann, D. B., Smerdon, M. J. and Springer, D. L. (1992) *Carcinogenesis* 1529.
19 Smith, R. D., Loo, J. A., Edmonds, C. G., Barinaga, C. J. and Udseth, H. R. (1990) *Anal. Chem.* **62**, 882–899.
20 McLuckey, S. A., Van Berkel, G. J. and Glish, G. L. (1990) *J. Am. Chem. Soc.* **112**, 5668–5670.

21 McLuckey, S. A. and Habibi-Goudarzi, S. (1993) *J. Am. Chem. Soc.* **115**, 12085–12095.
22 Little, D. P., Chorush, R. A., Speir, J. P., Senko, M. W., Kelleher, N. L. and McLafferty, F. W. (1994) *J. Am. Chem. Soc.* **116**, 4893–4897.
23 Bruce, J. E., Van Orden, S. L., Anderson, G. A., Hofstadler, S. A., Sherman, M. G., Rockwood, A. L. and Smith, R. D. (1995) *J. Mass Spectrom.* **30**, 124–133.
24 Wunschel, D. S, Fox, K. F., Fox, A., Bruce, J. E., Muddiman, D. C. and Smith, R. D. (1996) *Rapid Commun. Mass Spectrom.* **10**, 29–35.
25 Cheng, X., Gale, D. C., Udseth, H. R. and Smith, R. D. (1995) *Anal. Chem.* **67**, 586–593.
26 Fuerstenau, S. D., Benner, W. H. (1995) *Rapid Commun. Mass Spectrom.* **9**, 1508–1538.
27 Smith, R. D., Wahl, J. H., Goodlett, D. R. and Hofstadler, S. A. (1993) *Anal. Chem.* **65**, 574A–584A.
28 Speir, J. P., Senko, M. W., Little, D. P., Loo, J. A. and McLafferty, F. M. (1995) *J. Mass Spectrom.* **30**, 39–42.
29 Liu, C., Wu, Q., Harms, A. C. and Smith, R. D. submitted for publication.
30 Koleske, A. K. and Young, R. A. (1994) *Nature* **368**, 466.
31 Conaway, R. C. and Conaway, J. W. (1993) *Rev. Biochem.* **62**, 161.
32 Smith, L. M. (1993) *Science* **262**, 530.
33 Hunkapiller, T., Kaiser, R. J., Koop, B. F. and Hood, L. (1991) *Science* **254**, 59.
34 Olson, M. V. (1993) *Proc. Natl Acad. Sci. USA* **90**, 4338.
35 Billings, P. R., Smith, C. L. and Cantor, C. R. (1991) *FASEB J.* **5**, 28.